arXiv:0706.0124v2 [astro-ph] 30 Aug 2007

Influence of the Magnetic Coupling Process on the Advection Dominated Accretion Flows around Black Holes

Ren-Yi Ma, Feng Yuan

Shanghai Astronomical Observatory, Chinese Academy of Sciences, 80 Nandan Road, Shanghai 200030, China; Joint Institute for Galaxy and Cosmology (JOINGC) of SHAO and USTC; Email: ryma@shao.ac.cn; fyuan@shao.ac.cn

and

Ding-Xiong Wang

Department of Physics, Huazhong University of Science and Technology,Wuhan, 430074, China; Email: dxwang@hust.edu.cn

ABSTRACT

A large-scale closed magnetic field can transfer angular momentum and energy between a black hole (BH) and its surrounding accretion flow. We investigate the effects of this magnetic coupling (MC) process on the dynamics of a hot accretion flow (e.g., an advection dominated accretion flow, hereafter ADAF). The energy and angular momentum fluxes transported by the magnetic field are derived by an equivalent circuit approach. For a rapidly rotating BH, it is found that the radial velocity and the electron temperature of the accretion flow decrease, whereas the ion temperature and the surface density increase. The significance of the MC effects depends on the value of the viscous parameter α. The effects are obvious for $\alpha = 0.3$ but nearly ignorable for $\alpha = 0.1$. For a BH with specific angular momentum, $a_* = 0.9$, and $\alpha = 0.3$, we find that for reasonable parameters the radiative efficiency of a hot accretion flow can be increased by $\sim 30\%$.

Subject headings: accretion, accretion disks — magnetic fields — black hole physics

1. Introduction

As a variant of Blandford-Znajek (BZ) process (Blandford & Znajek 1977), the magnetic coupling (MC) between the central rotating black hole (BH) and its surrounding accretion disks has received much attention (e.g. Blandford 1999; Li & Paczýnski 2000; Li 2002;

Wang et al. 2002). By virtue of the large-scale closed magnetic field lines that connect the BH and its surrounding disk, the MC process conveys energy and angular momentum between the BH and the disk. Li (2002) showed that in the standard disk (SSD, Shakura & Sunyaev 1973; Novikov & Thorne 1973; Page & Thorne 1974) case the MC process may change the local radiative flux significantly.

Apart from SSD, ADAF is another important model of the accretion flow (Narayan & Yi 1994, 1995; Abramowicz et al. 1995; see Narayan, Mahadevan & Quataert 1998 and Kato, Fukue & Minesh 1998 for reviews). It has been applied to a number of accreting BH systems and successfully explains their spectral characteristics (see Narayan 2005 and Yuan 2007 for recent reviews). In ADAF models the thickness of the accretion flow is of the same order as radius, i.e. $H \sim r$, which means the large-scale field is easier to form in an ADAF than in a SSD (Tout & Pringle 1996; Livio et al. 1999). So it is interesting to investigate the influences of the MC process on an ADAF. Very recently, Ye et al. (2007) discussed this problem based on the self-similar solution of the ADAF. In this paper, we investigate the influences of the MC process on ADAFs through global solutions.

To properly assess the dynamical effects of large-scale magnetic fields on the accretion flow, one needs to obtain the fluids and the fields at the same time by solving the transfield equation, which is a nontrivial nonlinear partial differential equation with singular surfaces and free functions (Uzdensky 2004, 2005). An alternative way is MHD simulations (e.g. Hawley 2000; Hawley & Balbus 2002; Koide 2003; De Villiers et al. 2003; McKinney & Gammie 2004; Hirose et al. 2004). However, both of these approaches are complicated. Lai (1998) and Lee (1999a, b) adopted a phenomenological approach to research the magnetic coupling between the neutron star and its surrounding slim disk. They specified an ansatz for the magnetic fields and then numerically solve the basic equations of the accretion flow. In their model the disk is geometrically thin, $\partial/\partial r \sim 1/r \ll 1/H \sim \partial/\partial z$, and so the expressions of electromagnetic forces can be much reduced by omitting $\partial/\partial r$ terms. However, an MCADAF is thick and the expression of the electromagnetic force is complex. Here for simplicity we treat the MC process as a source of energy and angular moment without considering the radial and vertical components of the electromagnetic force in the momentum equations.

We derive the energy and angular momentum fluxes in the Kerr metric by using the approach of equivalent circuit (Macdonald & Thorne 1982). But for simplicity a pseudo-Newtonian potential of a rotating black hole given by Mukhopadhyay (2002) is adopted when we solve the solutions of the accretion flow.

In Section 2, we describe the MCADAF model and calculate the energy and angular momentum fluxes transferred by the magnetic field. In Section 3, we write down the basic equations describing the MCADAF. The numerical results are presented in Section 4 and Section 5 is devoted to a summary and discussions. Throughout this paper the geometric units c=G=1 are used.

2. MCADAF Model

We assume the ADAF is stationary and axisymmetric. The ADAF extends from the outer edge, r_{out}, to the BH horizon r_H. There are two kinds of magnetic fields in this model, i.e., large-scale closed magnetic field that connects the BH with the ADAF and small-scale tangled magnetic field, with the former contributing to the MC process and the latter to the viscosity. We assume these two kinds of fields work independently. If not mentioned we refer the magnetic field as the large-scale closed one hereafter. The region between the BH and the ADAF is assumed to be ideally conducting and force-free.

The field lines are supposed to distribute in the ranges of (r_H, r_{out}) on the disk and $(0, \theta_0)$ on the horizon. Due to the lack of knowledge about the magnetic field around the BH, we assume that the field threading the BH is constant, i.e. $B_H(\theta) = const.$ The field threading the ADAF is assumed to decrease with r following a power law form, but within the marginally stable orbit, $\lesssim r_{ms}$, the radial velocity of the accretion flow increases much faster thus the filed is likely to increase with radius. Given this consideration, we assume the field has the following distribution,

$$B_z(r) = B_0 F(r) = \begin{cases} B_0 \exp(r/r_p - 1) & \text{for} \quad r_H < r \le r_p \\ B_0 (r/r_p)^{-n} & \text{for} \quad r_p < r \le r_{out} \end{cases} \tag{1}$$

Here $r_H = M\left(1 + \sqrt{1 - a_*^2}\right)$ denotes the radius of the BH horizon, a_* is the dimensionless spin parameter of the BH, and $r_p = r_H + \lambda(r_{ms} - r_H)$.

Moderski, Sikora & Lasota (1997) gave an estimation of B_H with the balance between the ram pressure of the falling material and the magnetic pressure, i.e., $B_H^2/8\pi \sim \rho \sim \dot{M}_D/\left(4\pi r_H^2\right)$. Since the ram pressure can be larger than the magnetic press, we introduce a parameter c_B to indicate the strength of the magnetic field threading the horizon as

$$B_H = c_B \sqrt{2\dot{M}}/r_H, \quad 0 \le c_B \lesssim 1. \tag{2}$$

In the following derivation of this subsection, the Boyer-Lindquist coordinates are used. Assume all the field lines threading the BH are connected with the disk, then from the conservation of magnetic flux we have

$$\Psi = \int B_H (\rho\varpi)_H d\theta d\phi = \int B_z \left(\frac{\rho\varpi}{\sqrt{\Delta}}\right)_D dr d\phi, \tag{3}$$

where the subscripts "H" and "D" are used to indicate the quantities on the horizon and the equatorial plane of the disk ($\theta = \pi/2$), respectively. The Boyer-Lindquist coordinates are given as

$$\begin{aligned} &\Sigma^2 = (r^2 + a_*^2 M^2)^2 - a_*^2 M^2 \Delta \sin^2\theta, \quad \rho^2 = r^2 + a_*^2 M^2 \cos^2\theta, \\ &\Delta = r^2 + a_*^2 M^2 - 2Mr, \quad \varpi = (\Sigma/\rho)\sin\theta. \end{aligned} \tag{4}$$

Since $\Delta = 0$ at $r = r_H$, the lower boundary of the integration interval in the second equality is set to be $r_H + \delta r$, where δr is a small quantity and taken as $\delta r = 0.01$[1]. Substituting equation (1) into equation (3) we get

$$B_0 = \frac{\int B_H (\rho\varpi)_H d\theta d\phi}{\int F(r) \left(\frac{\rho\varpi}{\sqrt{\Delta}}\right)_D dr d\phi} = \frac{2Mr_H (1 - \cos\theta_0) B_H}{\int F(r) \left(\frac{\rho\varpi}{\sqrt{\Delta}}\right)_D dr d\phi} = 2r_H k(a_*, n) B_H / M. \tag{5}$$

Given the configuration of the field, we can derive the energy and angular momentum flux in the MC process by using the modified equivalent circuit approach (Wang et al. 2002). Considering a loop corresponds to two adjacent flux surfaces (characterized by the magnetic flux Ψ and $\Psi + \Delta\Psi$), the electromotive force due to the rotation of the BH and the disk are expressed as

$$\Delta\varepsilon_H = (\Delta\Psi/2\pi)\,\Omega_H, \quad \Delta\varepsilon_D = -\,(\Delta\Psi/2\pi)\,\Omega, \quad \Delta\Psi = 2\pi(\varpi\rho)_H \Delta\theta \cdot B_H. \tag{6}$$

The minus sign in the expression of $\Delta\varepsilon_D$ arise from the direction of the flux. The parameter Ω is the angular velocity of the ADAF, $\Omega_H = a_*/(2r_H)$ is the angular velocity of the BH horizon.

The equivalent surface resistivity of the BH horizon is 4π (Macdonald & Thorne 1982; Thorne et al. 1986), while the surface resistivity of the disk is $\sim 1/(H\sigma) = 4\pi\eta/H$, where $\eta \equiv 1/(4\pi\sigma)$ is the diffusivity of the magnetic field. As in many papers (e.g. Lubow et al. 1994; Lovelace et al. 1995; Soria et al. 1997), we assume η to be of the same order as the Shakura-Sunyaev (1973) kinematic α-viscosity coefficient, i.e., $\eta \sim \nu = \alpha c_s H$. The resistances of the annular ring on the horizon and the disk are thus

---

[1] The influence of δr can be ascribed to c_B as the effects of the MC process are mainly determined by the strength of the field in the region $r > r_p$ (we will show this in Sec.4).

$$\Delta Z_H = 4\pi \cdot \frac{\rho_H \cdot \Delta\theta}{2\pi\varpi_H} = \frac{2\rho_H \cdot \Delta\theta}{\varpi_H}, \tag{7}$$

$$\Delta Z_D = \frac{1}{H\sigma} \cdot \frac{\Delta r}{2\pi\varpi_D} = \frac{2\alpha c_s \cdot \Delta r}{\varpi_D}. \tag{8}$$

Thus the current in the loop is

$$\begin{aligned} &I = \tfrac{\Delta\varepsilon_H+\Delta\varepsilon_D}{\Delta Z_H+\Delta Z_D} = \left(\tfrac{\Delta\Psi}{2\pi}\right)\tfrac{\Omega_H-\Omega}{\Delta Z_H\cdot(1+\xi)} = \tfrac{1}{1+\xi}\cdot\tfrac{a_*(1-\beta_{HD})}{2\csc^2\theta-1+\sqrt{1-a_*^2}}\cdot MB_H. \\ &\left(\xi \equiv \tfrac{\Delta Z_D}{\Delta Z_H} = \tfrac{\alpha c_s\varpi_H}{\rho_H\varpi_D}\left|\tfrac{\Delta r}{\Delta\theta}\right|; \qquad \beta_{HD} \equiv \tfrac{\Omega}{\Omega_H}\right) \end{aligned} \tag{9}$$

In order to obtain ξ and I we have to find the value of $\Delta r/\Delta\theta$, which is related to the mapping relation between the angular coordinate on the horizon and the radial coordinate on the disk, i.e. $\theta(r)$. According to the conservation of the magnetic flux between the adjacent two flux surfaces,

$$d\Psi = B_H \cdot 2\pi\left(\varpi\rho\right)_H d\theta = -B_z \cdot 2\pi\left(\varpi\rho/\sqrt{\Delta}\right)_D dr. \tag{10}$$

Substitute equations (1) and (5) into the above equation, we get

$$M\frac{d\cos\theta}{dr} = k(a_*, n)\frac{\sqrt{r^4 + M^2a_*^2r^2 + 2M^3a_*^2r}}{M\sqrt{r^2 + a_*^2M^2 - 2Mr}}F(r) \equiv G(a_*, r, n). \tag{11}$$

Integrate equation (11) and we obtain the mapping relation:

$$\cos\theta = \cos\theta_0 + \int_{r_H}^{r} G(a_*, r, n) \cdot\ dr. \tag{12}$$

Our calculations show that, for the ADAF, the ratio of the height to radius around r_H is $\lesssim 0.3$, thus we assume $\theta_0 = 0.4\pi$ so that $cot\theta_0 \approx 0.3$. Substitute equation (11) into equation (9) we have

$$\xi = \frac{2\alpha c_s G(a_*, r, n)^{-1}}{\sqrt{r^2 + a_*^2M^2 + 2M^3a_*^2r^{-1}}\left[2\csc^2\theta - 1 + \sqrt{1 - a_*^2}\right]} \tag{13}$$

Since the current I on the BH horizon feels Ampere's force, the BH exerts a net torque on the magnetic flux tube

$$\Delta T_{MC} = \varpi B_H I\rho\Delta\theta = \left(\frac{\Delta\Psi}{2\pi}\right) I = \frac{4a_*(1-\beta_{HD})G(a_*, r, n)r_H}{(1+\xi)\left(2\csc^2\theta - 1 + \sqrt{1-a_*^2}\right)} \cdot MB_H^2 \cdot \Delta r. \tag{14}$$

From the second equality it is easy to find that this torque equals to the torque exerted on the disk by the same flux tube, or equivalently speaking, the angular momentum flows between the BH and the disk. The angular momentum flux can be written as

$$H_{MC} = \frac{1}{4\pi r}\frac{\Delta T_{MC}}{\Delta r}. \tag{15}$$

The power transmitted to the disk through the tube is given by

$$\Delta P_{MC} = I\Delta\varepsilon_D + I^2\Delta Z_D = 4\pi r H_{MC}\Omega\Delta r + 4\pi r H_{MC}(\Omega_F - \Omega)\Delta r \equiv \Delta P_{MW} + \Delta Q_{Ohm}, \tag{16}$$

where

$$\Omega_F = \frac{\Omega_H \Delta Z_D + \Omega\Delta Z_H}{\Delta Z_H + \Delta Z_D}, \tag{17}$$

is the angular velocity of the magnetic filed lines, $\Delta P_{MW} \equiv 4\pi r H_{MC}\Omega\Delta r$ is the rate of the mechanical work done by the electromagnetic torque on the disk and $\Delta Q_{Ohm} \equiv 4\pi r H_{MC}(\Omega_F - \Omega)\Delta r$ is the rate of Ohmic heating in the disk.

It is easy to calculate the power dissipated on the BH's stretched horizon intersecting with the flux tube:

$$\Delta Q_{BH} = I^2\Delta Z_H, \tag{18}$$

which increases the irreducible mass of the BH.

3. Basic Equations of the Accretion Flow

We assume the energy and angular momentum transferred by the MC process deposit into the accretion flow homogeneously in the vertical direction. The height-averaged basic equations describing the MCADAF can be written as

$$\dot{M} = -4\pi r\rho H\upsilon = const, \tag{19}$$

$$\upsilon\frac{d\upsilon}{dr} = (\Omega^2 - \Omega_K^2)r - \frac{1}{\rho}\frac{dp}{dr}, \tag{20}$$

$$\dot{M}\frac{d}{dr}(\Omega r^2) + 4\pi r H_{MC} = -\frac{d}{dr}\left(4\pi r^2\tau_{r\varphi}H\right), \tag{21}$$

$$\rho\upsilon T_i\frac{ds_i}{dr} = (1-\delta)(q^+_{vis} + \frac{Q_{Ohm}}{2H}) - q_{ie}, \tag{22}$$

$$\rho v T_e \frac{ds_e}{dr} = \delta(q^+_{vis} + \frac{Q_{Ohm}}{2H}) + q_{ie} - q^-. \tag{23}$$

Here $\dot{M}$ is the accretion rate, $c_s \equiv \sqrt{p/\rho}$ is the isothermal sound speed, $p = p_{gas}/\beta_t = \rho c_s^2/\beta_t$ is the total pressure of the tangled magnetic field and the gas pressure, β_t is the ratio of the gas pressure to the total pressure and is fixed at its "typical" value $\beta_t = 0.9$, T is the temperature, s is the entropy. The subscripts "i" and "e" indicate the quantities for ions and electrons, respectively. The quantity $\tau_{r\varphi} = -\alpha p$ is the $r\varphi$ component of the viscous stress tensor adopting the α prescription (Shakura & Sunyaev 1973), $H = c_s/\Omega_K$ is the vertical scale height, Ω_K is the Keplerian angular velocity calculated by using the pseudo-Newton potential given by Mukhopadhyay (2002), δ describes the fraction of the total energy that directly heats the electrons and is set to be $\delta = 0.3$ following the detailed modeling result to the supermassive black hole in our Galactic center (Yuan, Quataert & Narayan 2003), $q^+_{vis} = r\tau_{r\varphi}(d\Omega/dr)$ is the heating rate of the viscosity, q_{ie} represents the volume energy transfer rate from ions to electrons via Coulomb collisions, q^- is the cooling rate of the electrons, which consists of bremsstrahlung, synchrotron, and Comptonization (Narayan & Yi 1995; Manmoto et al. 1997), and $Q_{Ohm} = \Delta Q_{Ohm}/4\pi r\Delta r = H_{MC}(\Omega_F - \Omega)$ is the rate of Ohmic dissipation per unit area of the disk.

Adopting the no-torque boundary condition at the horizon, we integrate equation (21) from r_H to r and get the conservation equation for the angular momentum

$$l + \frac{\alpha r c_s^2}{v} + \frac{1}{\dot{M}} T^*_{MC}(r) = N_0, \tag{24}$$

where

$$T^*_{MC}(r) \equiv \int_{r_{out}}^{r} \frac{\partial T_{MC}}{\partial r} dr, \tag{25}$$

$$N_0 = l_0 + \frac{1}{\dot{M}} T^*_{MC}(r_H) = const, \tag{26}$$

with l_0 being the angular momentum per unit mass swallowed by the BH. The three terms on left-hand side of equation (24) correspond to the advected angular momentum, viscous torque and magnetic torque due to the field lines in the range from r to r_{out}.

One more relation is given by the equation of state,

$$p_{gas} = k(T_i/\mu_i + T_e/\mu_e)/m_u, \tag{27}$$

where μ is the mean molecular weight, k is the Boltzmann's constant, and m_u is the atomic mass unit.

Thus we have a set of six equations including one integral, two algebraic, and three differential equations, i.e. equations (19), (20), (22)-(24), and (27) for six unknown quantities, H (or c_s), v, ρ, Ω, T_i, and T_e. This set of equations can be solved with three outer boundary conditions and some given parameters (we will specify them later). However, there is some difficulty in obtaining Ω from the integral equation, viz. equation (24). So we use the first-order approximation, $T^{*}_{MC}(r) \approx T^{*}_{MC}(r+\Delta r) - \partial T_{MC}/\partial r|_{r+\Delta r}\,\Delta r$.

4. Numerical Results

We adopt $M = 10M_{\odot}$ and $r_{out} = 10^{3}M$ in this paper. Regarding the outer boundary of the ADAF, the ion temperature T_i should be of the same order as the virial temperature, and the electron temperature T_e should be somewhat lower than T_i because of the radiation of the electrons. The angular velocity of the accreting flow should be sub-Keplerian (Narayan, Mahadevan & Quataert 1998). So we impose the boundary conditions as $T_i = 2 \times 10^{9}$K, $T_e = 1 \times 10^{9}$K, $\upsilon/c_s = 0.3$. At last, by adjusting the eigenvalue of the problem, N_0, we can obtain the global transonic solution, i.e., a solution that can pass through the sonic point smoothly.

The free parameters of our MCADAF model include a_{*}, c_B, λ, n, α, and $\dot{m}$, where $\dot{m} = \dot{M}/\dot{M}_{\rm Edd}$ with the Eddington accretion rate $\dot{M}_{\rm Edd} = 1.39 \times 10^{18}(M/M_{\odot}){\rm g}\cdot{\rm s}^{-1}$. The first parameter describes the spin of the BH, the next three are associated with the magnetic field, and the last two describe the ADAF.

Figure 1 shows the curve of $\xi(\equiv \Delta Z_D/\Delta Z_H)$ when $a_{*} = 0.9, n = 3, \lambda = 1$ (corresponding to $r_p = r_{ms}$), $c_B = 1$, $\alpha = 0.3$ and $\dot{m} = 0.01$. As the figure shows, the resistance of the disk is small compared with the resistance on the stretched horizon. Especially, at the outer boundary, the resistance of the disk is completely negligible. Since the distribution of the magnetic field we assumed is not smooth, there is a break at r_{ms}. Figure 2 shows the curves of Ω, Ω_F, Ω_H and $\Omega_F - \Omega$ for the same parameters as Figure 1. From this figure we find that Ω_F always lies between Ω_H and Ω, which agrees with equation (17). We also find that the relative angular velocity of the magnetic field lines to the disk, i.e. $\Omega_F - \Omega$, achieves maximum at some radius between the inner and outer boundaries. This is a natural result because $\Omega_F - \Omega$ is proportional to the product of two factors, $\Delta Z_D/(\Delta Z_H + \Delta Z_D)$ and $\Omega_H - \Omega$ (see equation (17)), which approach to zero at the outer and inner boundaries, respectively. At the innermost region, $\Omega > \Omega_H$. This unphysical result arise because we do not use the exact general relativity.

From Figure 3 we can get some ideas of the partitioning of the magnetically-extracted rotational energy of the BH. In this figure we show the curves of the rate of mechanical work due to electromagnetic torque and three kinds of heating rates per unit area. The solid line represents Q_{Ohm}, the long dashed line for $P_{MW} = \Delta P_{MW}/4\pi r\Delta r = H_{MC}\Omega$, the short dashed line for the Ohmic dissipation on the BH's stretched horizon, $Q_{BH} = \Delta Q_{BH}/4\pi r \Delta r$, while the dotted line for the viscous heating rate per unit area, $Q_{vis} = 2Hq^{+}_{vis}$. As the figure shows, Q_{Ohm} dominates over P_{MW} in the outer region of the disk while the latter dominates in the inner region. Compare $Q_{Ohm} + P_{MW}$ with Q_{BH}, we find the efficiency of extracting energy from the BH to the disk is very small except in the inner region. Moreover, it can be seen that the MC power is small in contrast to the viscous heating rate.

The profiles of the radial Mach number, surface density Σ, T_e and T_i, specific angular momentum l, and the advection factor f $(= q_{adv}/(q^{+}_{vis} + F_{MC}/2H))$ of the accretion flow for different c_B are shown in Figure 4. The solid, dotted, and dashed lines correspond to $c_B = 1$, 0.5, and 0, respectively.

From Figure 4 we find that, when the MC process is present, the sonic point moves inward, T_e decreases, Σ and T_i increase, while l and f decrease in the outer region and increase in the inner region. These effects can be understood as follows. As the spin of the BH is very fast ($a_* = 0.9$), angular momentum and energy are transferred from the BH to the disk. The energy flux raises the temperature of the ions. The angular momentum flux hinders the infalling of the accreting material. Thus the sonic point moves inward and the surface density increases. Since the optical depth is proportional to the surface density, the Compton cooling rate goes up, and consequently, the temperature of the electrons decreases. Compared with the case without MC process, the $r\varphi$ component of the viscous stress tensor in a MCADAF around a fast rotating BH is a bit larger due to the higher pressure p in the outer region, so the angular momentum is transferred more efficiently and the specific angular momentum there is smaller. But at small radius, the increase of the angular momentum due to the MC process dominates over the decrease due to the viscous torque, so that the specific angular momentum can even increase, as can be seen from equation (21). Similarly, in the outer region of the disk the radiative cooling rate becomes higher and f decreases, while in the inner region f goes up because the heating rate due to the MC process increases more quickly than the radiative cooling rate does. Additionally, as the magnetic field threading the BH becomes stronger, the influences of the MC process become more significant. However, as Figure 3 shows, the contribution of the MC process is of less importance, so its influences are small.

Figure 5 shows the influences of the parameter λ (ref. the paragraph below eq. 1). The solid and dashed lines are for $\lambda = 1$ and 1.5, respectively. For comparison purpose the dotted line is shown for the case without MC process. From this figure we see that the effects of increasing λ are similar to those of increasing c_B. This is because the magnetic field in the region $r > r_p$ strengthens as these two parameters increase. Although the increase of λ also leads to the decrease of the magnetic field in the region $r_H < r < r_p$, the MC effects are small in this region, because the gravitational force there is so strong and the radial velocity is so high that the energy and angular momentum transferred by the MC process do not play any significant role.

Figure 6 shows the effects of parameter n (ref. eq. 1). The solid and dashed lines are for $n = 4$ and 3, respectively. The lines for the case without MC process are shown with the dotted lines. From this figure we find that the MC effects are more significant for smaller n. It is because the magnetic field is weaker in the outer region ($r > r_p$) when n is bigger, which can be seen from equations (1) and (5).

We calculate the influence of the MC process on the radiative efficiency of the ADAF. The results are shown in Figure 7. The parameters are $a_* = 0.9, c_B = 1.0, \lambda = 1$ and $n = 3$. The quantity $\dot{M}_{crit}$ denotes the critical accretion rate of an ADAF, which is $\sim \alpha^2 \dot{M}_{\rm Edd}$ (e.g. Narayan, Mahadevan & Quataert 1998). The radiative efficiency increased by the MC process is written as $\eta_{\rm MC} = \eta_{\rm MCADAF} - \eta_{\rm ADAF}$, where $\eta_{\rm MCADAF}$ and $\eta_{\rm ADAF}$ are the efficiencies of the MCADAF and pure ADAF, respectively. From Figure 7 we find that, when $\alpha = 0.3$, the MC process can raise the efficiency by about one percentage point, i.e., $\sim 30\% \eta_{\rm ADAF}$. But when $\alpha = 0.1$ the effect of the MC process is very weak. The efficiency goes up because of two reasons: firstly, the MC process transports additional energy to the ADAF; secondly the angular momentum transported by the MC process decreases the radial velocity of the ADAF, and thus makes the ADAF more efficient in radiating. When α is smaller, the specific angular momentum of the accreting material is larger since viscosity is less efficient in moving angular momentum out, and consequently, the difference between the angular velocities of the BH and the disk is smaller. Considering equations (14), (15) and (16), the angular momentum and energy transported by the MC process decrease.

In all the above discussions, the spin of the BH is very large. The angular momentum and energy are transferred from the BH to the disk. If the BH rotates slowly, the angular momentum and energy may be transferred from the disk to the BH. However, since H_{MC} is proportional to a_*, the MC effect is not so significant as the case when $a_* = 0.9$. In addition, there is a critical value of a_*, at which the total energy and angular momentum transmitted by the MC process are zero and consequently $\eta_{MC} = 0$. In the SSD case this value is about $a_* = 0.283$ for $n = 3$ (Wang et al. 2003), whereas in our MCADAF model, it is about 0.172. The critical value is smaller in the MCADAF case because the angular velocity of the ADAF is sub-Keplerian.

The spin of the BH can even be negative, i.e., retrograde spin. From equations (14) and (15) it is easy to find that the angular momentum always flows from the ADAF to the BH when $a_* < 0$. If the resistance of the ADAF is zero, i.e. $\xi = 0$ or $\Omega_F = \Omega$, the energy flows in the same direction as that of the angular momentum, as can be seen from equation (16).

If ξ is nonzero and big enough, Ohmic dissipation in the disk may offset the loss of energy that conveyed to the BH. According to equation (16), the critical condition is $\Delta P_{MC} = 0$, or equivalently, $\xi + \beta_{HD} = 0$. Our calculations show that when $a_* < 0$, ξ is so small that $\xi + \beta_{HD} < 0$ holds for almost all cases, and the net energy flows from the ADAF to the BH. If the BH rotates rapidly, e.g. $a_* = -0.9$, the effects of the MC process will be negative compared to the case of $a_* = 0.9$: the radial velocity and the temperature of the electrons increase, the sonic point moves outward, the temperatures of the ions decrease, etc.

5. Summary and Discussion

In this paper we investigate the influence of the magnetic coupling process on the dynamics of the ADAF. The effects of the MC process on the basic equations of the accretion flow is simplified as a source of angular momentum and energy. The angular momentum and energy fluxes are derived with the equivalent circuit approach. We find that when the BH rotates fast (e.g., $a_* = 0.9$) and when the viscous parameter α is large, $\alpha = 0.3$, for reasonable magnetic field, the MC process can mildly affect the dynamics of the ADAF, increasing the ion temperature and the density of the accretion flow and decreasing the electron temperature and the radial velocity. The MC process can also raise the effciency of the ADAF by $\sim 30\%$. But if $\alpha = 0.1$ or smaller, the influences of the MC process are much weaker and can be neglected.

In the above calculations the strength of the magnetic field is estimated following Moderski, Sikora & Lasota (1997), which is equivalent to assume $c_B \leq 1$. Obviously uncertainties exist in the above estimation. On the one hand, recent MHD simulations show that the magnetic field strength near the horizon can be very high, almost four times as large as the the equipartition value (McKinney 2005), which corresponding roughly to $c_B \approx 2$. On the other hand, our calculation requires that there exists an upper limit to the value of c_B. This is because if c_B were too large, the transferred angular momentum from the BH to the accretion flow would be so significant that the accretion could not proceed due to the strong centrifugal force. We find that the highest value of c_B depends on the accretion rate for given a_*. It can be ~ 5 if the accretion rate is very low but ~ 1 if the accretion rate is as high as $\dot{m} \gtrsim 0.1$. Considering the above two limitations on c_B, the increased efficiency due to the MC process $\eta_{\rm MC} (\equiv \eta_{\rm MCADAF} - \eta_{\rm ADAF})$ can be as high as 10%.

Observations of the hard state of BH X-ray binaries sometimes show luminosities as high as $L_x \sim 10 - 30\% L_{\rm Edd}$, which are much higher than $4\% L_{Edd}$, the highest luminosity that an ADAF surrounding a Schwarzschild BH can produce (Esin et al. 1997). When the accretion rate is higher than the critical rate of an ADAF, the accretion flow enters into the regime of the Luminous Hot Accretion Flow (LHAF) (Yuan 2001). Yuan et al. (2007) found that the highest luminosity an LHAF surrounding a non-rotating BH (with $\dot{M} = 0.3\dot{M}_{\rm Edd}$) can produce was $\sim 8\% L_{\rm Edd}$, which is still too low. They speculated that when the spin of the BH and the MC process were taken into account, the highest luminosity an LHAF could produce would possibly be high enough to explain the observed high L_x. Now, taking into account the black hole spin and the MC process, we recalculate the maximum luminosity an LHAF (with $\dot{m} = 0.3$) can produce, with reasonable parameters such as $a_* = 0.9$, $\lambda = 1, c_B \approx 1$ (note this is the largest possible value when $\dot{m} = 0.3$) and $n = 3$. We find the highest luminosity is $\sim 14\% L_{\rm Edd}$. The increase due to the MC process is $\sim 1.0\% L_{\rm Edd}$ while that due to the BH spin is $\sim 5.1\% L_{\rm Edd}$. So the MC process seems not so helpful to increase the highest luminosity an LHAF can produce to explain the observed highest L_x.

In this paper we assume that the closed field extends to the outer boundary of the ADAF according to a power law. As a matter of fact the magnetic connection between the BH and the disk can be maintained only within a limited radius. Wang et al. (2004) discussed the constraint of the screw instability to the MC region of a SSD based on the Kruskal-Shafranov criterion: the screw instability will occur, if the magnetic field line turns around itself about once (Kadomtsev 1966; Bateman 1978). It turns out that the MC region is limited within some critical radii on the SSD. By numerically solving the Grad-Shafranov equation, the main differential equation that describes the structure of the magnetosphere, Uzdensky (2005) argued that for a rapidly-rotating BH the field lines are frame-dragged by the BH so much, and the toroidal magnetic field becomes so strong that the magnetic connection between the BH and the disk cannot be maintained over a large range of radii on the disk. We shall address this issue in the context of ADAF in our further work.

We thank the anonymous referee for his/her very constructive suggestions and careful examination, which greatly improve the presentation. This work was supported by the One-Hundred-Talent Program of CAS and the Pujiang Program.

REFERENCES

Abramowicz, M. A., Chen, X., Kato, S., Lasota, J.-P., & Regev, O. 1995, ApJ, 438, L37

Bateman, G. 1978, in MHD Instabilities (Cambridge: MIT)

Blandford, R. D., & Znajek, R. L. 1977, MNRAS, 179, 433

Blandford, R. D. 1999, in Astrophysical Discs, ed. J. A. Sellwood, & J.Goodman, ASP Conf. Ser., 160, 265 (astro-ph/9902001)

De Villiers, J., Hawley, J. F., & Krolik J. H. 2003, ApJ, 599, 1238

Esin, A. A., McClintock, J. E., & Narayan, R. 1997, ApJ, 489, 865

Hawley, J. F. 2000, ApJ, 528, 462

Hawley, J. F., & Balbus, S. A. 2002, ApJ, 573, 738

Hirose, S., Krolik, J. H., De Villiers, J., & Hawley, J. F. 2004, ApJ, 606, 1083

Kato, S., Fukue, J., & Mineshige, S., eds. 1998, Black-Hole Accretion Disks, (Tyoto: Kyoto Univ. Press)

Kadomtsev, B. B. 1966, Rev. Plasma Phys., 2, 153

Koide, S. 2003, Phys. Rev. D, 67, 104010

Lai, D. 1998, ApJ, 502, 721

Lee, U. 1999a, ApJ, 511, 359

Lee, U. 1999b, ApJ, 525, 386

Li, L. X., & Paczynski, B. 2000, ApJ, 534, L197

Li, L. X. 2002, ApJ, 567, 463

Livio, M., Ogilvie, G. I., & Pringle, J. E. 1999, ApJ, 512, 100

Lovelace, R.V.E., Romanova, M.M., & Bisnovatyi-Kogan, G. S. 1995 MNRAS, 275, 244

Lubow, S. H., Papaloizou, J. C. B., & Pringle, J. E., 1994, MNRAS, 267, 235

Macdonald, D., & Thorne, K. S. 1982, MNRAS, 198, 345

Manmoto, T., Mineshige, S., & Kusunose, M. 1997, ApJ, 489, 791

McKinney, J. C. 2005, ApJ, 630, L5

McKinney, J. C., & Gammie, C. F. 2004, ApJ, 611, 977

Moderski, R., Sikora, M., & Lasota, J. P. 1997, in Proceedings of the International Conf., Relativistic Jets in AGNs, ed. M. Ostrowski, M. Sikora, G. Madejski, & M. Begelman (astro-ph/9706263)

Mukhopadhyay, B. 2002, ApJ, 581, 427

Narayan, R. 2005, ApS&S, 300, 177

Narayan, R., & Yi, I., 1994, ApJ, 428, L13

Narayan, R., & Yi, I. 1995, ApJ, 452, 710

Narayan, R., Mahadevan, R., & Quataert, E. 1998, in ”The Theory of Black Hole Accretion Discs”, eds. M. A. Abramowicz, G. Bjornsson, and J. E. Pringle, (Cambridge University Press)

Novikov, I. D., & Thorne, K. S., in Black Holes, ed. C. DeWitt and B. DeWitt (New York: Gordon & Breach), 345

Page, D. N., & Thorne, K. S., 1974, ApJ, 191, 499

Shakura, N. I., Sunyaev, R. A. 1973, A&A24, 337

Soria, R., Li, J., & Wickramasinghe, D. T. 1997, ApJ, 487, 769

Thorne, K. S., Price, R. H., & Macdonald, D. A. 1986, in Black Holes: The Membrane Paradigm, (New Haven and London: Yale Univ Press)

Tout, C. A., & Pringle, J. E. 1996, MNRAS, 281, 219

Uzdensky, D. A. 2004, ApJ, 603, 652

Uzdensky, D. A. 2005, ApJ, 620, 889

Wang, D. X., Xiao, K., & Lei, W. H. 2002, MNRAS, 335, 655

Wang, D. X., Lei, W. H., & Ma, R. Y. 2003, MNRAS, 342, 851

Wang, D. X., Ma, R. Y., Lei, W. H., & Yao, G. Z. 2004, ApJ, 601, 1031

Ye, Y. C., Wang, D. X., & Ma, R. Y. 2007, New A, 12, 471

Yuan, F. 2001, MNRAS, 324, 119

Yuan, F. 2007, to appear in ”The Central Engine of Active Galactic Nuclei”, ed. L. C. Ho and J.-M. Wang (San Francisco: ASP) (astro-ph/0701638)

Yuan, F., Quataert, E., & Narayan, R. 2003, ApJ, 598, 301

Yuan, F., Zdziarski, A. A., Xue, Y. Q., & Wu, X. B. 2007, ApJ, 659, 541

This preprint was prepared with the AAS LaTeX macros v5.2.

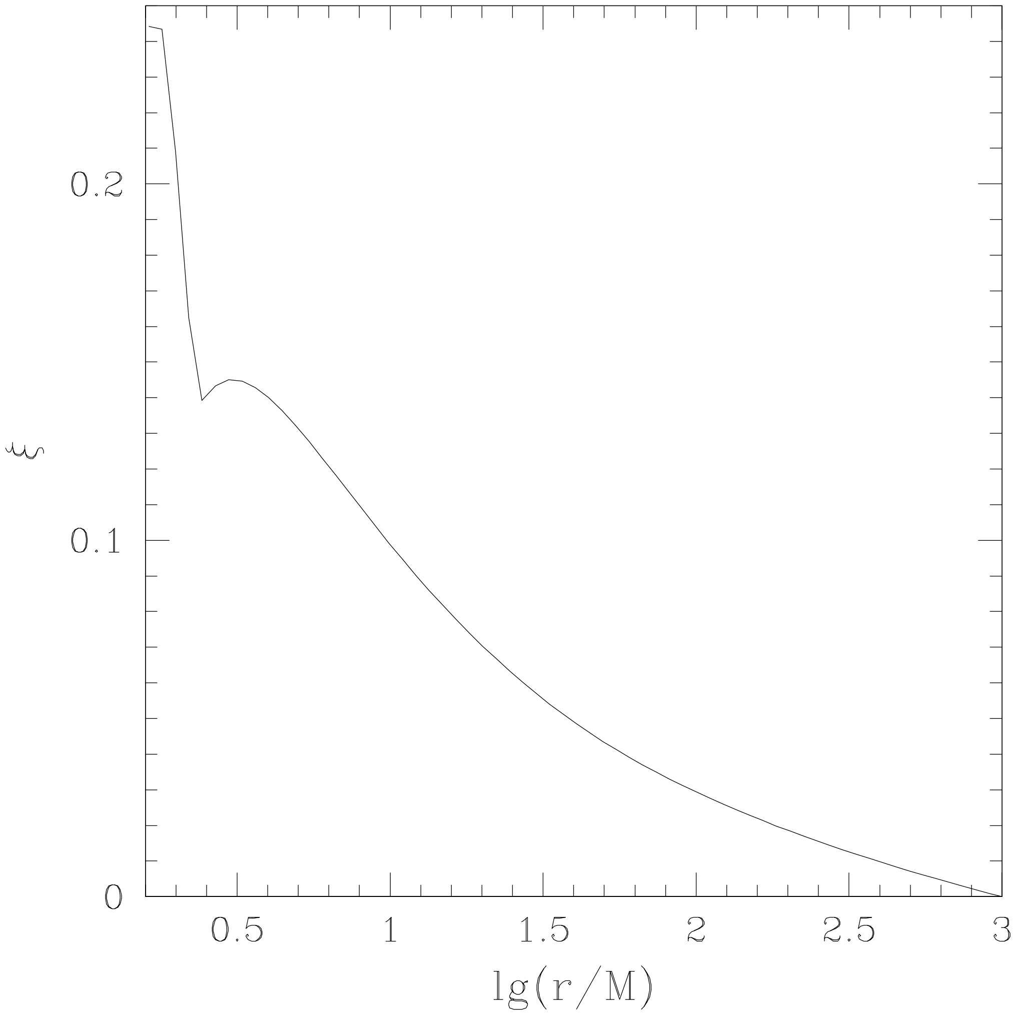

Fig. 1.— Profile of $\xi(\equiv \Delta Z_D/\Delta Z_H)$ on the disk. The parameters are $a_* = 0.9, n = 3, \lambda = 1$ (corresponding to $r_p = r_{ms}$), $c_B = 1$, $\alpha = 0.3$ and $\dot{m} = 0.01$.

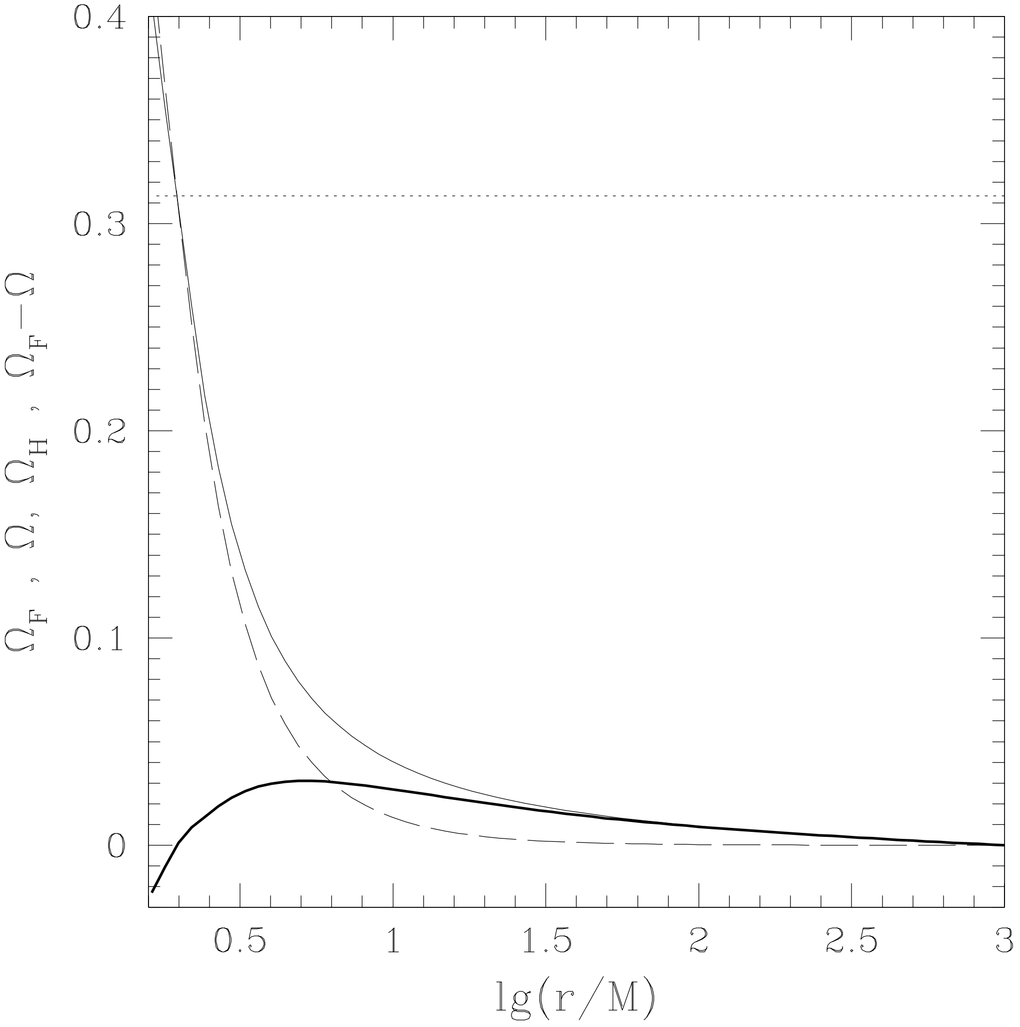

Fig. 2.— Curves of the angular velocities. The solid, dashed and dotted lines correspond to Ω_F, Ω and Ω_H, respectively. The thick solid line shows $\Omega_F - \Omega$. The parameters are the same as Figure 1.

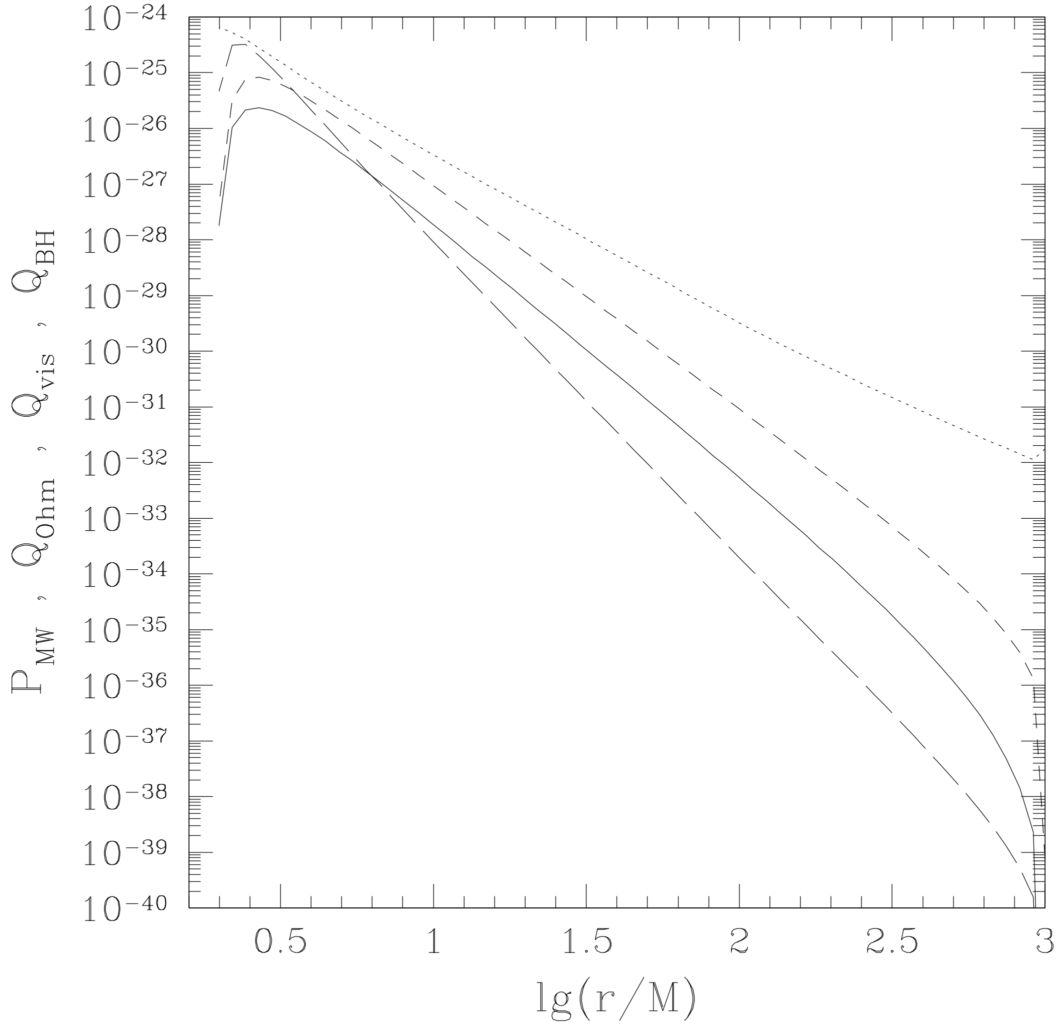

Fig. 3.— Curves of the rate of mechanical work due to electromagnetic torque and the heating rates per unit area. The solid line represents the rate of Ohmic heating in the disk Q_{Ohm}, the long dashed line shows the power of the electromagnetic torque on the disk P_{MW}, the short dashed line shows the Ohmic dissipation on the BH's stretched horizon Q_{BH}. As comparison the curve of viscous heating rate per unit area Q_{vis} is shown in dotted line. The parameters are the same as Figure 1.

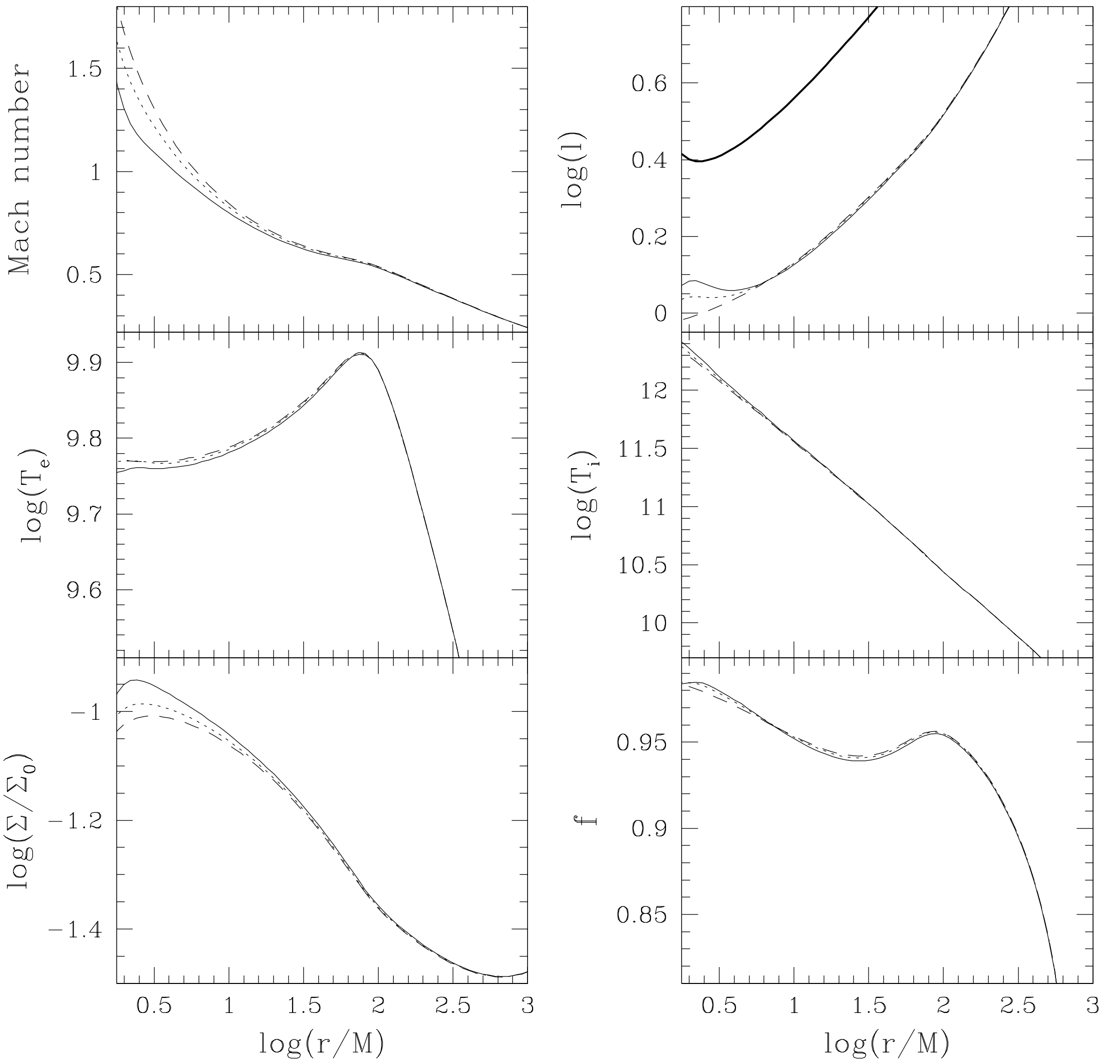

Fig. 4.— The profiles of the radial Mach number, specific angular momentum l, electron and ion temperatures T_e and T_i, surface density Σ (in unit of $\Sigma_0 \equiv \dot{M}/M$), and the advection factor f for different c_B. Other parameters are the same as Figure 1. The solid, dotted, and dashed lines correspond to $c_B = 1$, 0.5, and 0, respectively. The thick solid line in the top right panel shows the Keplerian angular momentum.

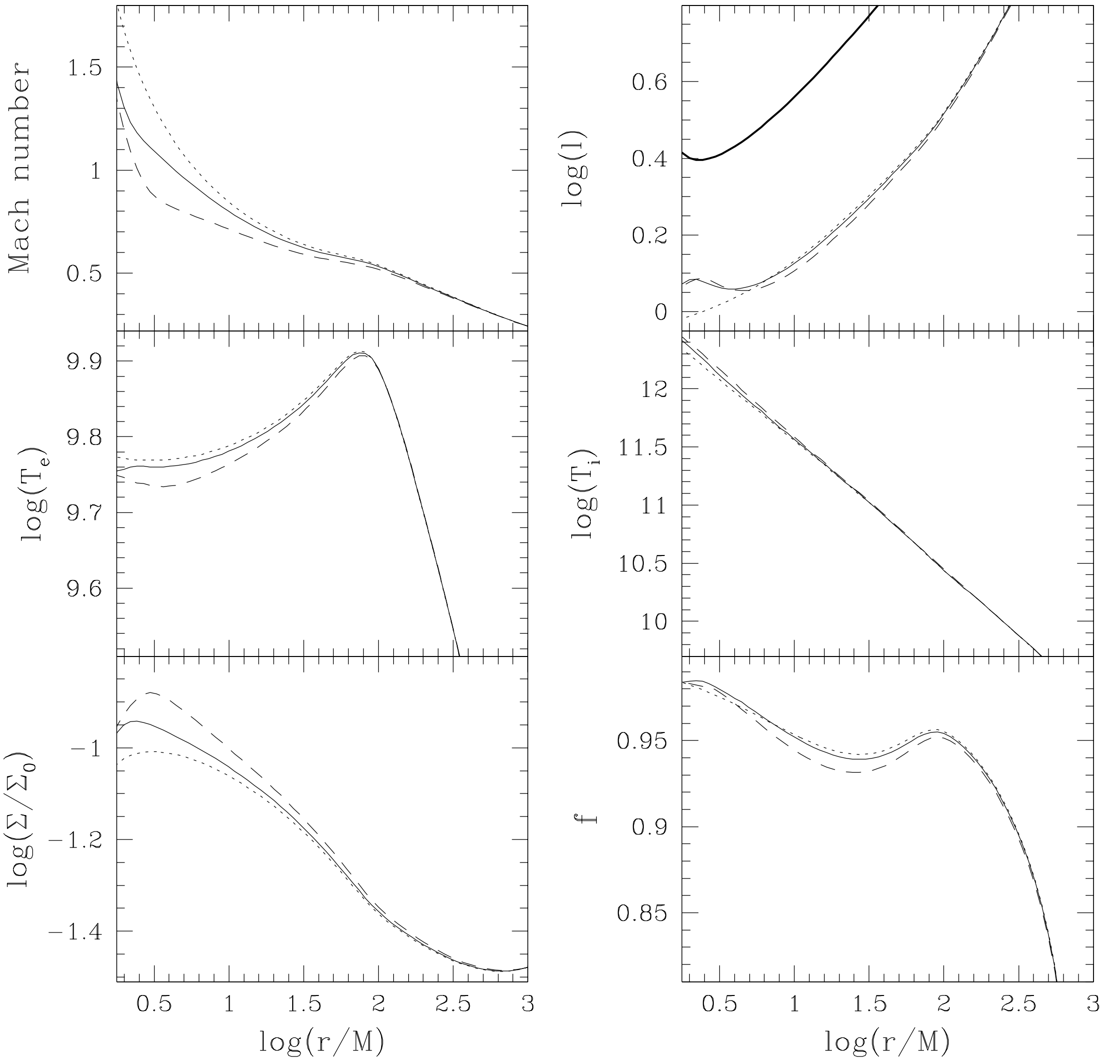

Fig. 5.— Same with Figure 1, but for different λ when $a_* = 0.9$, $c_B = 1$, $\alpha = 0.3$, and $\dot{m} = 0.01$. The solid and dashed lines correspond to $\lambda = 1$ and 1.5, respectively. The dotted line corresponds to the case without MC process.

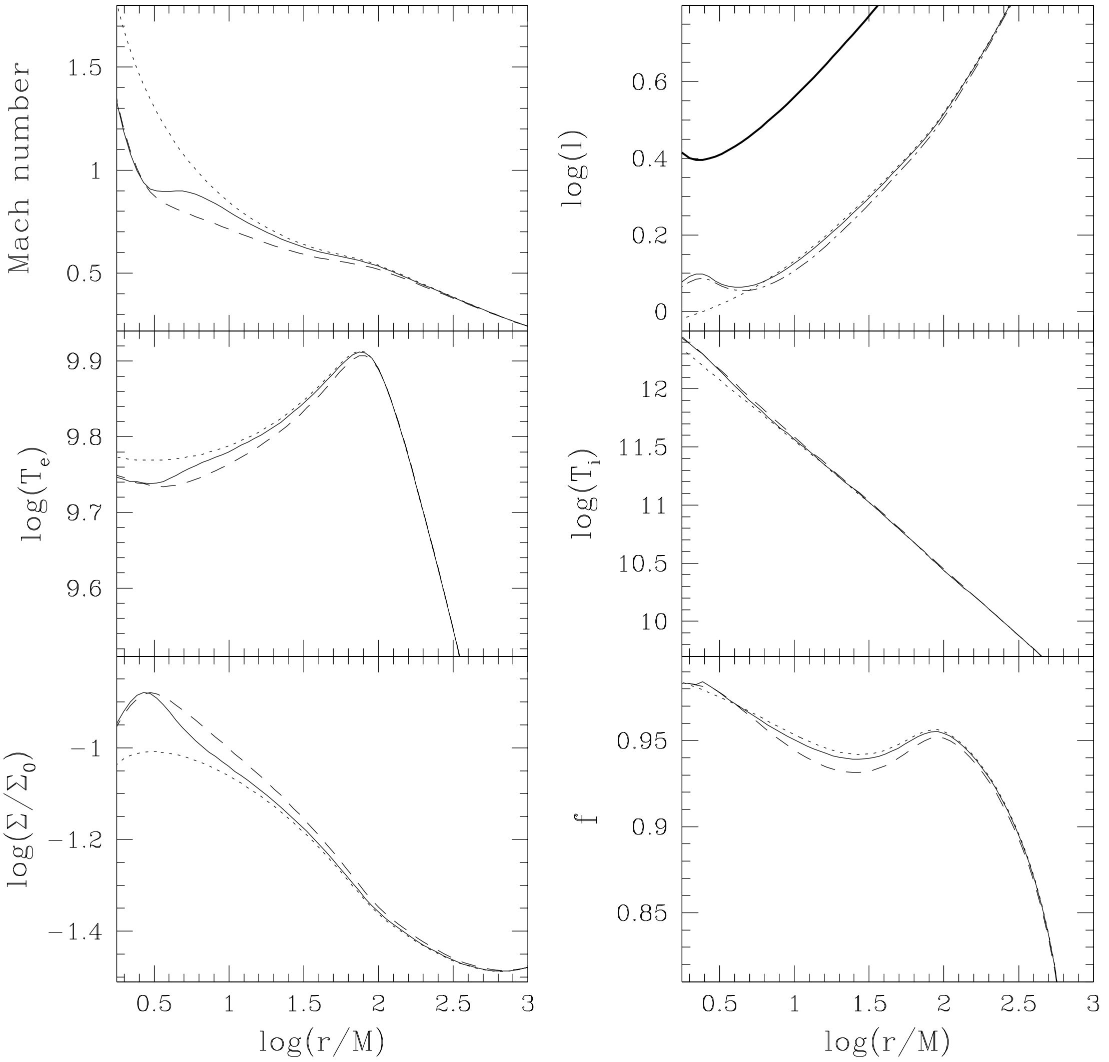

Fig. 6.— Same with Figure 1, but for different n when $a_* = 0.9$, $c_B = 1$, $\alpha = 0.3, \lambda = 1.5$, and $\dot{m} = 0.01$. The solid and dashed lines correspond to $n = 4$ and 3, respectively. The dotted line corresponds to the case without MC process.

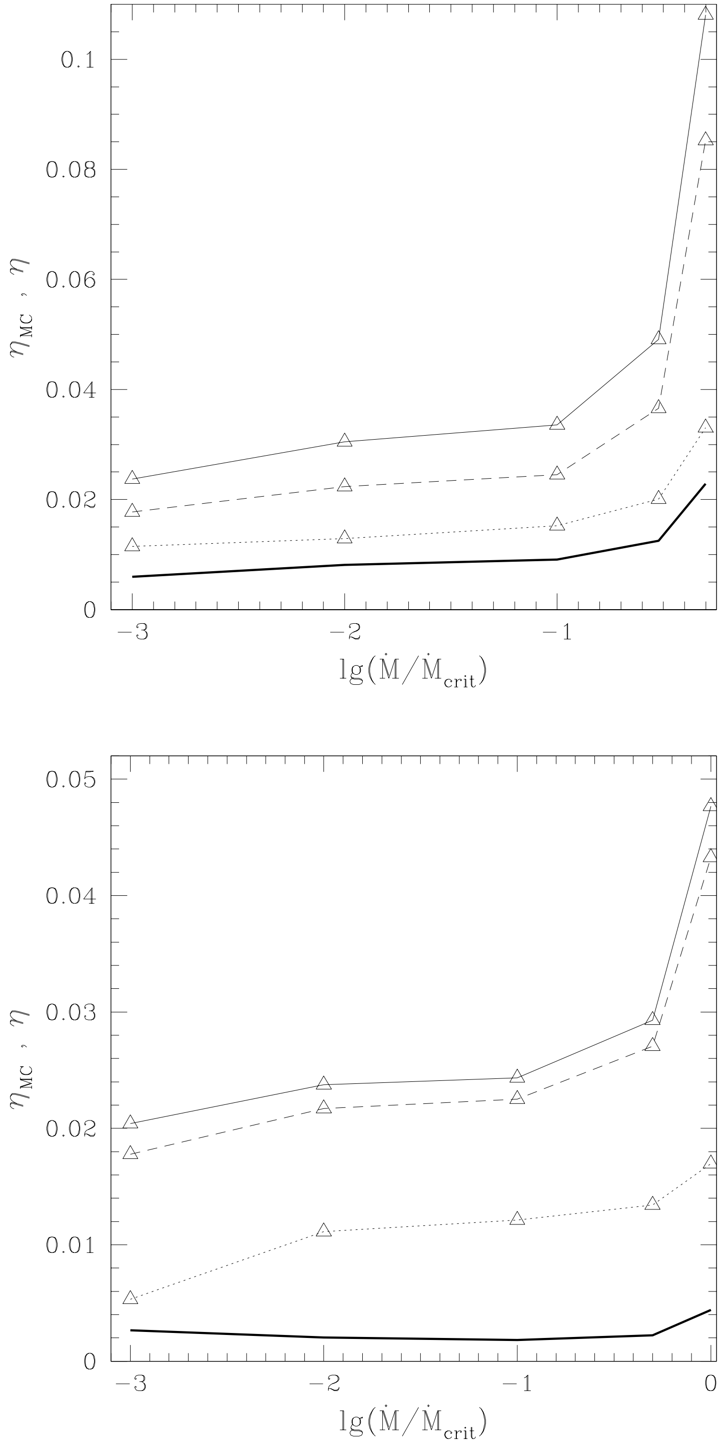

Fig. 7.— The radiative efficiency of the accretion flow as a function of the accretion rate. Here $\dot{M}_{\rm crit} \equiv \alpha^2 \dot{M}_{\rm Edd}$. The thin solid lines correspond to the results of the present MCADAF model ($a_* = 0.9$, $c_B = 1.0$, $\lambda = 1.0$ and $n = 3$), the dashed lines indicate the results without MC process, the thick solid lines show the efficiency improved by the MC process (η_{MC}), and the dotted lines show the results of a Schwarzschild BH without considering the MC process. In the upper panel $\alpha = 0.3$ and in the lower panel $\alpha = 0.1$.